Cell

A PP2A Regulatory Subunit Regulates *C. elegans* Insulin/IGF-1 Signaling by Modulating AKT-1 Phosphorylation

Srivatsan Padmanabhan,[1,3] Arnab Mukhopadhyay,[1,3,4] Sri Devi Narasimhan,[1,3] Gregory Tesz,[2] Michael P. Czech,[2] and Heidi A. Tissenbaum[1,2,*]
[1]Program in Gene Function and Expression
[2]Program in Molecular Medicine
University of Massachusetts Medical School, 364 Plantation Street, Worcester, MA 01605, USA
[3]These authors contributed equally to this work
[4]Present address: National Institute of Immunology, Aruna Asaf Ali Marg, New Delhi 110067, India
*Correspondence: heidi.tissenbaum@umassmed.edu
DOI 10.1016/j.cell.2009.01.025

SUMMARY

The *C. elegans* insulin/IGF-1 signaling (IIS) cascade plays a central role in regulating life span, dauer, metabolism, and stress. The major regulatory control of IIS is through phosphorylation of its components by serine/threonine-specific protein kinases. An RNAi screen for serine/threonine protein phosphatases that counterbalance the effect of the kinases in the IIS pathway identified *pptr-1*, a B56 regulatory subunit of the PP2A holoenzyme. Modulation of *pptr-1* affects IIS pathway-associated phenotypes including life span, dauer, stress resistance, and fat storage. We show that PPTR-1 functions by regulating worm AKT-1 phosphorylation at Thr 350. With striking conservation, mammalian B56β regulates Akt phosphorylation at Thr 308 in 3T3-L1 adipocytes. In *C. elegans*, this ultimately leads to changes in subcellular localization and transcriptional activity of the forkhead transcription factor DAF-16. This study reveals a conserved role for the B56 regulatory subunit in regulating insulin signaling through AKT dephosphorylation, thereby having widespread implications in cancer and diabetes research.

INTRODUCTION

The insulin/IGF-1-like signaling (IIS) pathway is an evolutionarily conserved neuroendocrine pathway that regulates metabolism, development, stress resistance, and life span (Antebi, 2007; Barbieri et al., 2003; Kenyon, 2005; Wolff and Dillin, 2006). In *Caenorhabditis elegans* (*C. elegans*), the insulin-like receptor DAF-2 (Kimura et al., 1997) signals through a PI 3-kinase (AGE-1/AAP-1) (Morris et al., 1996; Wolkow et al., 2002) signaling cascade that activates the downstream serine/threonine kinases PDK-1, AKT-1, AKT-2, and SGK-1 (Hertweck et al., 2004; Paradis et al., 1999; Paradis and Ruvkun, 1998). These kinases in turn function to negatively regulate the forkhead transcription factor (FOXO), DAF-16 (Lin et al., 1997; Ogg et al., 1997).

Reduction-of-function mutations in serine/threonine kinases upstream of DAF-16 lead to changes in life span, development, metabolism, and/or stress resistance (Antebi, 2007; Kenyon, 2005; Wolff and Dillin, 2006). Importantly, loss-of-function mutations in *daf-16* completely suppress these phenotypes (Antebi, 2007; Kenyon, 2005; Mukhopadhyay et al., 2006; Wolff and Dillin, 2006). Thus, DAF-16 is a major downstream target of the IIS pathway. Regulation of DAF-16 by AKT-1, AKT-2, and SGK-1 results in its nuclear exclusion and sequestration in the cytosol (Lin et al., 2001) (Hertweck et al., 2004; Lee et al., 2001). In contrast, under low signaling conditions, active DAF-16 enters the nucleus and transactivates or represses its direct target genes (Henderson and Johnson, 2001; Hertweck et al., 2004; Lee et al., 2001; Lin et al., 2001; Oh et al., 2006). Strikingly, this negative regulation of FOXO/DAF-16 is conserved across species. In mammals, the AKT and SGK kinases can phosphorylate and negatively regulate FOXO (Brunet et al., 1999; Brunet et al., 2001).

Although regulation of the IIS pathway by serine/threonine protein kinases has been extensively studied, little is known about the phosphatases acting in this pathway. In *C. elegans*, the lipid phosphatase DAF-18 (homologous to mammalian Phosphatase and Tensin Homolog, PTEN) is the only phosphatase that has been identified and characterized as a negative regulator of the IIS pathway (Gil et al., 1999; Mihaylova et al., 1999; Ogg and Ruvkun, 1998; Rouault et al., 1999). The increased life span of *daf-2* mutant worms is suppressed by loss-of-function mutation in *daf-18* (Dorman et al., 1995; Larsen et al., 1995). Therefore, to identify additional regulators of the IIS pathway, we performed a directed RNAi screen of serine/threonine protein phosphatases that affect phenotypes regulated by the IIS pathway.

C. elegans development proceeds from an egg, through four larval stages into a self-fertilizing, hermaphrodite adult. However, under unfavorable growth conditions such as crowding and low food availability, worms enter a stage of diapause known as dauer (Riddle et al., 1997). Upon favorable growth

A

Phosphatase family	Members	*C. elegans* homologs
PPM	PP2C	10
	PDP	1
PPP	PP1	3
	PP2A	1
	PP2B	1
	PP4	2
	PP5	1
	PP6	1
	PP1 like	40
PP2A regulatory subunits	B55/PR55	1
	B56/PR61	2
	B72/PR72	4

C

Experiment	RNAi	% Dauer ± Std. Dev.	(n)
1	vector	54.4 ± 4.9	285
	daf-18	0.3 ± 0.5	312
	fem-2	0.0 ± 0.0	388
2	vector	17.5 ± 3.7	405
	daf-18	0.0 ± 0.0	395
	pptr-1	1.3 ± 1.6	470

B

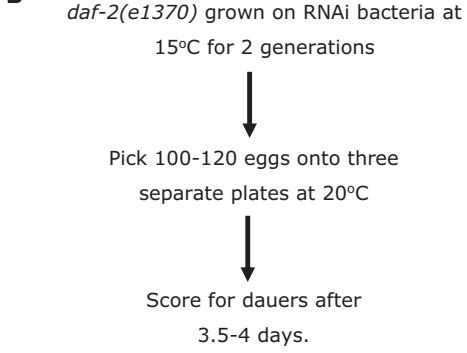

D

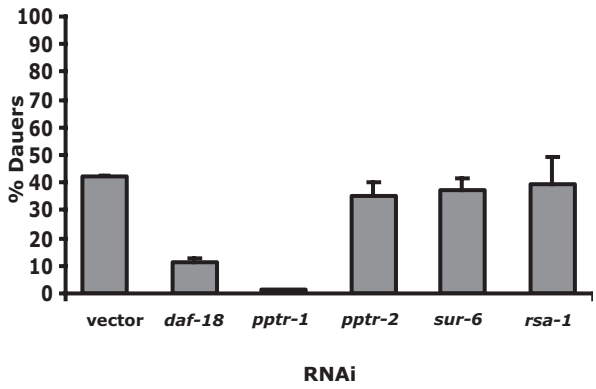

Figure 1. *pptr*-1, a Regulatory Subunit of the PP2A Holoenzyme, Was Identified as a Top Candidate in a Directed RNAi Screen to Identify Serine/Threonine Phosphatases that Regulate the IIS Pathway

(A) The different families and classes of the phosphatases included in the RNAi screen.

(B) A schematic representation of the RNAi screen. All the assays were performed in triplicate.

(C) The top two candidates that dramatically suppressed *daf-2(e1370)* dauer formation at 20°C (*fem-2*, and *pptr-1*). Both *fem-2* and *pptr-1* RNAi were able to suppress *daf-2* dauer formation to a similar level as *daf-18* RNAi. Error bars indicate the standard deviations among the different RNAi plates within one experiment. Data shown [% Dauers ± Std. Dev. (n)] are from one representative experiment.

(D) *pptr-1* is the only PP2A regulatory subunit family member that dramatically suppresses *daf-2(1370)* dauer formation. Error bars indicate the standard deviations among the different RNAi plates within one experiment. Data shown are from one representative experiment.

conditions, dauers are able to form reproductive adults. Since worms form dauers constitutively when the function of IIS pathway is reduced by mutations, we took advantage of a temperature-sensitive (ts) allele of *daf-2* for the RNAi screen (Riddle et al., 1981). We screened for genes that suppressed dauer formation in *daf-2(e1370)* mutants. In this report, we characterize PPTR-1, a regulatory subunit of the PP2A holoenzyme, as an important regulator of development, longevity, metabolism, and stress response in *C. elegans*. We show that PPTR-1 acts by modulating AKT-1 phosphorylation and as a consequence controls DAF-16 activity.

RESULTS

RNAi Screen to Identify Phosphatases in the IIS Pathway

To identify the serine/threonine phosphatases in the *C. elegans* genome, we performed in silico analyses using both NCBI KOGs (clusters of euKaryotic Orthologous Groups) and WormBase (a *C. elegans* database: http://www.wormbase.org; WS152) annotations. A total of 60 genes were identified for further analysis (Figure 1A). We obtained RNAi clones for these phosphatases from the Ahringer RNAi library (Kamath et al., 2003), generated them using available clones from the ORFeome library (Reboul et al., 2003), or cloned them de novo using Gateway Technology (Invitrogen, USA; Experimental Procedures). We were unable to clone three of the phosphatase cDNAs and therefore screened a total of 57 candidates.

In addition, we included six of the seven annotated PP2A holoenzyme regulatory subunits (one was not cloned) in the screen for two reasons. First, a preliminary chemical inhibitor screen identified the PP2A family of phosphatases as important regulators of DAF-16 nuclear translocation (S.P. and H.A.T., unpublished data). Second, the PP2A holoenzyme is comprised of a catalytic, a structural, and a regulatory subunit (Janssens et al., 2008), and RNAi of the catalytic and structural subunits of PP2A resulted in lethality (data not shown).

daf-2(e1370) carries a mutation in the insulin receptor tyrosine kinase domain that results in a ts phenotype for dauer formation (Kimura et al., 1997). *daf-2(e1370)* worms arrest as 100% dauers at 25°C, whereas at 15°C they have a normal reproductive cycle

Table 1. Epistasis Analysis of Dauer Formation Using Different IIS Pathway Mutants Grown on RNAi Clones

Strains	Percent Dauer ± Standard Deviation (n)		
	Vector RNAi	*daf-18* RNAi	*pptr-1* RNAi
daf-2(e1368)[a]	69.2% ± 9.4% (202)	0% (295)	3.8% ± 4.4% (257)
daf-2(e1370)[b]	17.2% ± 5.9% (517)	0.2% ± 0.3% (397)	9.6% ± 7.3% (460)
daf-2(e1370);daf-3(mgDf90)	94.5% ± 0.8% (589)	40.4% ± 14.0% (308)	42.7% ± 14.6% (329)
pdk-1(sa680)[a]	95.6% ± 1.0% (490)	80.8%[c] (52)	9.5% ± 0.3% (180)
daf-2(e1370)	73.0% ± 0.2% (525)	3.5% ± 1.7% (279)	4.1% ± 3.8% (344)
daf-2(e1370);akt-1(ok525)[d]	94.8% ± 3.1% (237)	1.0% ± 0.3% (386)	96.0% ± 1.7% (186)
daf-2(e1370);akt-2(ok393)	36.8% ± 3.8% (336)	5.0% ± 1.1% (610)	10.8% ± 4.3% (583)
daf-2(e1370)	79.1% ± 5.4% (601)	0.7% ± 1.0% (405)	27.2% ± 14.8% (536)
daf-2(e1370);sgk-1(ok538)	65.4% ± 4.9% (338)[e]	0.3% ± 0.4% (303)	0% (364)

All strains were maintained at 15°C and assays performed at 20°C unless otherwise indicated. Also, dauer formation of all strains was scored after 3.5–4 days unless otherwise indicated. Data shown are representative of one experiment.

[a] The experiment was performed at 25°C.

[b] Dauers were scored after 5 days.

[c] In most experiments, the *pdk-1(sa680)* worms failed to hatch on *daf-18* RNAi. This number represents 20% of the eggs picked for this assay.

[d] Dauers were scored after 7–8 days. For *daf-2(e1370);akt-1(ok525)* worms on vector or *pptr-1* RNAi, all of the nondauers were either partial dauers or dauer-like. They did not develop into adults even after 2 weeks.

[e] Dauers were scored after 7–8 days. The *daf-2(e1370);sgk-1(ok538)* strain shows a gro phenotype, and worms remain at the L1/L2 stage for 6–7 days at 20°C.

(Riddle et al., 1997). At an intermediate temperature of 20°C, a significant percentage of *daf-2(e1370)* worms form dauers. Therefore, at this temperature, one can use RNAi to easily assess the contribution of any gene in modulating *daf-2* dauer formation.

For the screen, *daf-2(e1370)* mutants were grown on RNAi-expressing bacteria for two generations, and eggs were picked onto three plates for each RNAi clone (Figure 1B). The plates were incubated at 20°C and scored 3.5–4 days later for the presence of dauers and nondauers. Since DAF-18 is the only known phosphatase that negatively regulates the IIS in *C. elegans*, we used *daf-18* RNAi as a positive control in all of our experiments. From a total of 63 RNAi clones (57 phosphatases and six regulatory subunits), we identified two phosphatases that dramatically decreased *daf-2(e1370)* dauer formation to a level similar to *daf-18* RNAi (Figure 1C).

Our top candidate, *fem-2* (T19C3.4), functions in *C. elegans* sex determination (Kimble et al., 1984; Pilgrim et al., 1995). However, further analysis with an additional *daf-2* allele, *daf-2(e1368)*, revealed that *fem-2* RNAi suppresses dauer formation in an allele-specific manner. *fem-2* RNAi suppressed dauer formation of *daf-2(e1370)* but not *daf-2(e1368)* (data not shown), and therefore we focused on the next top candidate.

pptr-1 (W08G11.4), the next candidate, is a member of the B56 family of genes encoding regulatory subunits of the PP2A protein phosphatase holoenzyme. The *C. elegans* genome contains seven known PP2A regulatory subunit genes (*pptr-1* and *pptr-2*, B56 family; *sur-6*, B55 family; F47B8.3, C06G1.5, *rsa-1*, and T22D1.5, B72 family; currently F47B8.3 is not annotated as a PP2A regulatory subunit according to WormBase Release WS194). To determine the specificity of *pptr-1* in regulating dauer formation, we retested the six PP2A regulatory subunits included in the screen for their ability to regulate dauer formation in *daf-2(e1370)* mutants. Knockdown efficiency of each RNAi clone was verified by RT PCR (Table S1A available online). As shown in Figure 1D and Tables S1A and S1B, only *pptr-1* RNAi suppressed *daf-2(e1370)* dauer formation comparable to *daf-18* RNAi.

We next analyzed the effect of *pptr-1* RNAi on dauer formation of *daf-2(e1368)*. *pptr-1* RNAi significantly suppressed the dauer formation of *daf-2(e1368)* (69.2% ± 9.4% on vector RNAi versus 3.8% ± 4.4% on *pptr-1* RNAi; Table 1 and Table S2). Therefore, the effect of *pptr-1* RNAi on *daf-2* mutants is not allele specific. Together, these results indicate that *pptr-1* may function downstream of *daf-2*. In addition, *pptr-1* is the only PP2A regulatory subunit to affect *daf-2* dauer formation.

pptr-1 Regulates Dauer Formation through the IIS Pathway

To further investigate the role of *pptr-1* in dauer formation, we performed genetic epistasis analysis. In addition to the *C. elegans* IIS pathway, a second parallel TGF-β pathway also regulates dauer formation (Patterson and Padgett, 2000; Savage-Dunn, 2005). In this pathway, loss-of-function mutations in *daf-7* (TGF-β ligand), *daf-1*, and *daf-4* (receptors) or *daf-14* and *daf-8* (R-Smads) lead to constitutive dauer formation; loss-of-function mutations in *daf-3* (Co-Smad) or *daf-5* (Sno/Ski) suppress these phenotypes (da Graca et al., 2004; Gunther et al., 2000; Inoue and Thomas, 2000; Patterson et al., 1997; Ren et al., 1996). However, mutations in *daf-3* do not suppress *daf-2(e1370)* dauer formation (Vowels and Thomas, 1992). We generated a *daf-2(e1370);daf-3(mgDf90)* double mutant, which bears a null mutation in *daf-3* (Patterson et al., 1997) and essentially removes the input from the TGF-β pathway for dauer formation. In this strain, the dauer formation of *daf-2(e1370); daf-3(mgDf90)* worms was suppressed by *pptr-1* RNAi (94.5% ± 0.8% dauers on vector RNAi to 42.7% ± 14.6% dauers on *pptr-1* RNAi; Table 1 and Table S2). These data suggest that *pptr-1* controls dauer formation specifically through the IIS pathway and not the TGF-β pathway.

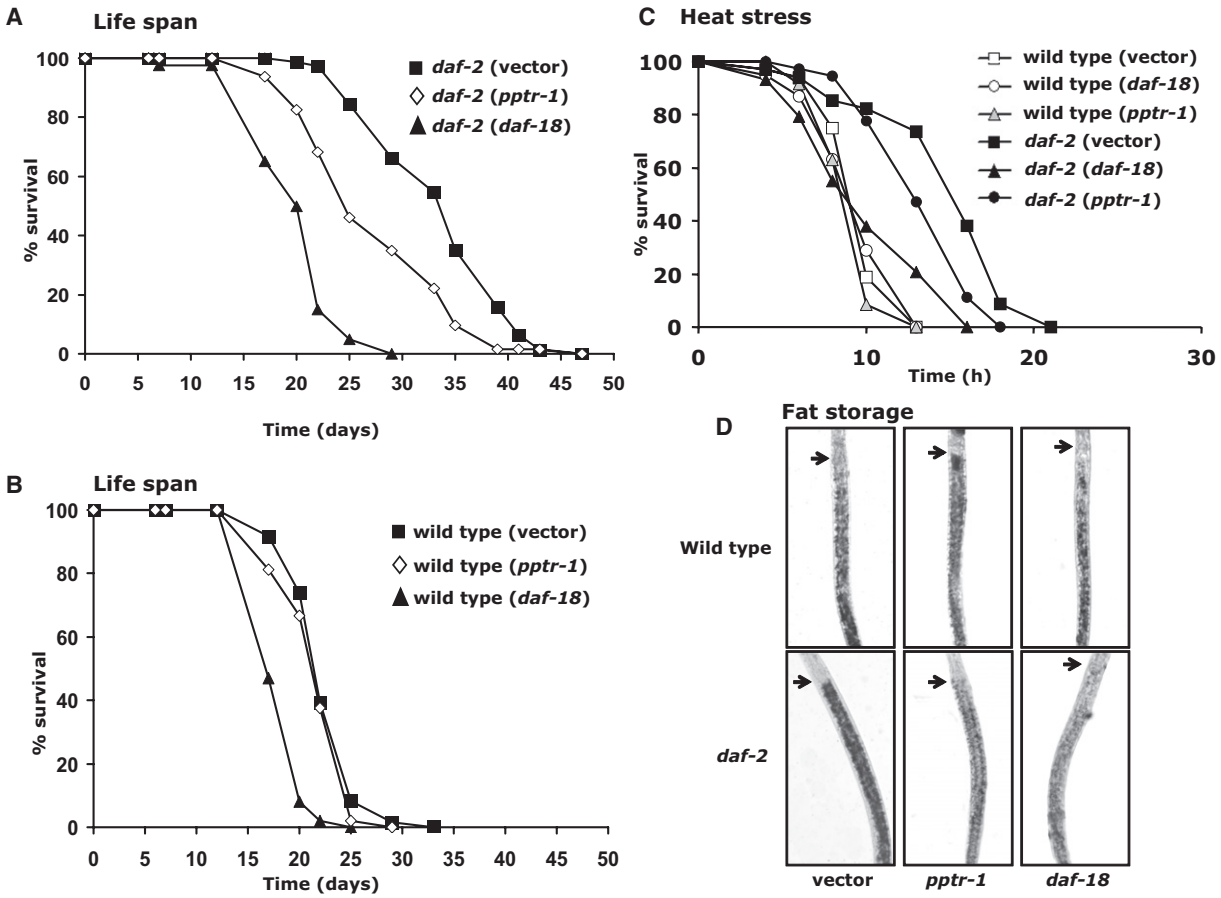

Figure 2. *pptr-1* Regulates Life Span, Thermotolerance and Fat Storage through the IIS Pathway

Data shown are from one representative experiment.

(A) *pptr-1* RNAi significantly reduces the life span of *daf-2(e1370)* mutants similar to *daf-18* RNAi. Mean life span [days ± SD (n)] of *daf-2(e1370)* is as follows: on vector RNAi, 33.9 ± 0.7 days (n = 77); on *pptr*-1 RNAi, 27.7 ± 0.9 days (n = 63), $p < 0.0001$; and on *daf-18* RNAi, 20.4 ± 0.6 days (n = 40), $p < 0.0001$.

(B) *pptr-1* RNAi does not affect the life span of wild-type worms. Mean life span [days ± SD (n)] of wild-type worms is as follows: on vector RNAi, 22.8 ± 0.4 days (n = 61); and on *pptr*-1 RNAi, 21.9 ± 0.5 days (n = 49). *daf-18* RNAi reduces mean life span of wild-type worms to 18.6 ± 0.3 days (n = 48), $p < 0.0001$.

(C) The thermotolerance of *daf-2(e1370)* worms is reduced by *pptr-1* as well as *daf-18* RNAi; mean survival [hours ± SD (n)] of *daf-2(e1370)* worms at 37°C on vector RNAi was 15.2 ± 0.7 hr (n = 34), whereas on *pptr-1* RNAi the survival was 13.8 ± 0.5 hr ($p < 0.006$) (n = 36) and 10.3 ± 0.7 hr ($p < 0.0001$) (n = 29) on *daf-18* RNAi. *pptr-1* RNAi did not affect the thermotolerance of wild-type worms (mean survival was 9.8 ± 0.4 hr on vector RNAi [n = 32], 9.3 ± 0.3 hr on *pptr-1* RNAi [n = 35] and 9.7 ± 0.4 hr on *daf-18* RNAi [n = 32]).

(D) Sudan black staining showing that *pptr-1* RNAi reduces the increased fat storage of *daf- 2(e1370)* worms, similar to *daf-18* RNAi, but has no effect on wild-type fat storage. Arrows indicate the pharynx. A representative picture from one of three independent experiments (n = 30) is shown.

pptr-1 Affects Longevity, Metabolism, and Stress Response Downstream of the IIS Receptor

In addition to dauer formation, the *C. elegans* IIS pathway also regulates life span, fat storage, and stress resistance (Antebi, 2007; Kenyon, 2005; Wolff and Dillin, 2006). Since *pptr-1* regulates dauer formation specifically via the IIS pathway, we next determined whether this gene could also affect these other important phenotypes.

Mutations in *daf-2* result in life span extension (Kenyon et al., 1993) that is suppressed by loss-of-function mutations in *daf-18* (Dorman et al., 1995; Larsen et al., 1995). To investigate whether *pptr-1* can regulate life span similar to *daf-18*, we determined whether knockdown of *pptr-1* by RNAi could affect *daf-2(e1370)* life span. We grew wild-type and *daf-2(e1370)* worms on vector, *daf-18*, and *pptr-1* RNAi and measured life span (Figure 2A). Similar to *daf-18* RNAi, knockdown of *pptr-1* resulted in a significant reduction in *daf-2(e1370)* life span (mean life span of *daf-2(e1370)* on vector RNAi is 33.9 ± 0.7 days, on *pptr-1* RNAi is 27.7 ± 0.9 days, and on *daf-18* RNAi is 20.4 ± 0.6 days, $p < 0.0001$; Figure 2A and Table S3A). In contrast, life span of wild-type worms was unaffected by *pptr-1* RNAi (mean life span of wild-type worms is 22.8 ± 0.4 days on vector RNAi, 21.9 ± 0.5 days on *pptr-1* RNAi, and 18.6 ± 0.3 days on *daf-18* RNAi; Figure 2B and Table S3A). Thus, *pptr-1* affects life span in addition to dauer formation.

Life span extension correlates well with increased stress resistance (Lithgow and Walker, 2002; Oh et al., 2005). For example, *daf-2(e1370)* mutants are not only long-lived but are also

extremely resistant to various stresses such as heat and oxidative stress (Honda and Honda, 1999; Lithgow et al., 1995; Munoz and Riddle, 2003). Therefore, we next analyzed the effect of *pptr-1* RNAi on the thermotolerance of *daf-2(e1370)* mutants. As anticipated, *pptr-1* RNAi significantly reduced the thermotolerance of *daf-2(e1370)* mutants. [On vector RNAi, *daf-2(e1370)* had a mean survival of 15.2 ± 0.7 hr, whereas on *pptr-1* RNAi survival was 13.8 ± 0.5 hr ($p < 0.006$). *pptr-1* RNAi did not affect the thermotolerance of wild-type worms; mean thermotolerance was 9.8 ± 0.4 hr on vector RNAi, versus 9.3 ± 0.3 hr on *pptr-1* RNAi; Figure 2C and Table S4.]

In addition to enhanced life span and stress resistance, *daf-2* mutants have increased fat storage (Ashrafi et al., 2003; Kimura et al., 1997). We next asked whether *pptr-1* could also affect fat storage in wild-type and *daf-2(e1370)* worms by using Sudan black staining. Consistent with our life span and stress resistance results, *pptr-1* RNAi suppressed the increased fat storage of *daf-2(e1370)* without affecting wild-type fat storage (Figure 2D). Finally, *daf-2* mutants have a slow growth phenotype (Gems et al., 1998; Jensen et al., 2007) that is suppressed by knockdown of *daf-16* by RNAi (Table S5). Similar to *daf-16* RNAi and *daf-18* RNAi, *pptr-1* RNAi suppresses this slow growth phenotype. Together, these experiments suggest that *pptr-1* regulates multiple phenotypes associated with the IIS pathway in *C. elegans*.

pptr-1 Functions at the Level of *akt-1*

Signals from DAF-2 are transduced to the PI 3-kinase AGE-1 to activate the downstream serine/threonine kinase PDK-1. PDK-1 activates three downstream serine/threonine kinases, AKT-1, AKT-2, and SGK-1 (Antebi, 2007; Kenyon, 2005; Wolff and Dillin, 2006). These kinases together regulate the transcription factor DAF-16 by direct phosphorylation (Hertweck et al., 2004). Mutations in *daf-16* suppress the enhanced dauer formation of *pdk-1* (Paradis et al., 1999) or *akt-1/akt-2* mutants (Oh et al., 2005; Paradis and Ruvkun, 1998). Thus far, our analysis suggests that *pptr-1* functions in the IIS pathway. We sought to identify the potential target of *pptr-1* by performing genetic epistasis experiments on components of the IIS pathway.

First we analyzed the effect of *pptr-1* RNAi on dauer formation of a *pdk-1* mutant. Dauer formation of *pdk-1(sa680)* was suppressed by *pptr-1* RNAi (95.6% ± 1.0% dauers on vector RNAi versus 9.5% ± 0.3% dauers on *pptr-1* RNAi, Table 1 and Table S2). In contrast, *daf-18* RNAi had no effect on *pdk-1(sa680)* dauer formation (Table 1 and Table S2). Therefore, these results place *pptr-1* downstream of *pdk-1* and are consistent with the current understanding that *daf-18* acts upstream of *pdk-1*.

Next, to investigate whether *pptr-1* acts at the level of *akt-1*, *akt-2*, or *sgk-1*, we first analyzed dauer formation in *akt-1(ok525)*, *akt-2(ok393)*, and *sgk-1(ok538)* single mutants and the *akt-1(ok525);akt-2(ok393)* double mutant. While *akt-1(ok525)*, *akt-2(ok393)*, and *sgk-1(ok538)* single mutants do not arrest as dauers at either 20°C or 25°C, the *akt-1(ok525); akt-2(ok393)* double mutant forms 100% dauers at all temperatures (Oh et al., 2005). To circumvent this problem, we generated double mutants of *daf-2(e1370);akt-1(ok525)*, *daf-2(e1370);akt-2(ok393)*, and *daf-2(e1370);sgk-1(ok538)* and tested these strains for dauer formation on vector, *daf-18*, and *pptr-1* RNAi. We reasoned that in a *daf-2* mutant background, the *akt-1, akt-2*, and *sgk-1* mutants would exhibit temperature-induced dauer formation. Indeed, all three double mutants were able to form dauers at 20°C (Table 1 and Table S2—see panel for vector RNAi). Importantly, *pptr-1* RNAi significantly suppressed dauer formation in *daf-2(e1370);akt-2(ok393)* (36.8% ± 3.8% dauers on vector RNAi versus 10.8% ± 4.3% on *pptr-1* RNAi; Table 1 and Table S2). In addition, *pptr-1* RNAi suppressed dauer formation of *daf-2(e1370);sgk-1(ok538)* worms (65.4% ± 4.9% dauers on vector RNAi versus 0% on *pptr-1* RNAi, Table 1 and Table S2). In contrast, *pptr-1* RNAi did not affect dauer formation of *daf-2(e1370);akt-1(ok525)* mutants (vector RNAi is 94.8% ± 3.1% versus 96.0% ± 1.7% on *pptr-1* RNAi; Table 1 and Table S2). However, *daf-18* RNAi can suppress *daf-2(e1370);akt-1(ok525)* dauer formation (reduced to 10.5% ± 0.8%; Table 1). These observations genetically place *pptr-1* at the level or downstream of *akt-1* in the IIS pathway.

PPTR-1 and AKT-1 Are Expressed in the Same Tissues

Since *pptr-1* and *akt-1* genetically interact, we wanted to investigate whether they have a common expression pattern. We generated or obtained *akt-1::gfp*, *akt-2::gfp*, *sgk-1::gfp* transgenic worms, and we tagged *pptr-1* with *mCherry* and a minimal *flag* tag to generate *pptr-1::mCherry-flag* transgenic worms (henceforth referred to as *pptr-1::mC-flag;* Experimental Procedures; GFP/mC-FLAG refers to protein and *gfp/mC-flag* stands for transgene). We made double transgenic worms by crossing *pptr-1::mC-flag* worms to each of the above-mentioned GFP lines. Similar to published data, we observed AKT-1::GFP predominantly in the pharynx, several head neurons, the nerve ring, spermathecae, and vulva (Paradis and Ruvkun, 1998); AKT-2::GFP in the pharynx (predominantly in the anterior region), somatic muscles, vulva muscles, and spermathecae (Paradis and Ruvkun, 1998); and SGK-1::GFP in amphid neurons, intestine, and some tail neurons (Hertweck et al., 2004) (Figures 3A–3C, middle panel, and Figure S1). PPTR-1::mC-FLAG was also observed in the pharynx, head neurons, nerve ring, spermathecae, and vulva (Figures 3A–3C, left panel, and Figure S1). To observe the subcellular localization of PPTR-1, we stained *pptr-1::mC-flag* worms with DAPI (Experimental Procedures). We found that PPTR-1 is predominantly cytosolic with little DAPI overlap (Figure S2 and Movies S1–S8). As shown in Figures 3A–3C (Merge) as well as in the confocal movies (Movies S1–S8), there is remarkable overlap between the expression patterns of PPTR-1 and AKT-1. We also observed partial overlap between AKT-2::GFP and PPTR-1::mC-FLAG, predominantly in the pharynx (Figure 3B, Merge; Movies S1–S8). SGK-1 and PPTR-1 are expressed in different tissues, and we do not see any significant overlap (Figure 3C, Merge; Movies S1–S8).

PPTR-1 Regulates AKT-1 Phosphorylation

Given the genetic epistasis as well as the overlapping expression patterns, we next determined whether PPTR-1 directly interacts with AKT-1 by coimmunoprecipitation (co-IP) in *C. elegans*. For all biochemical experiments, we used the PD4251 strain as a control. This strain contains *Pmyo-3::gfp* with a mitochondrial localization signal and *Pmyo-3::lacZ-gfp* with a nuclear localization signal (Fire et al., 1998). This strain will be referred to as *myo-3::gfp*. We prepared lysates from mixed-stage *akt-1::gfp;*

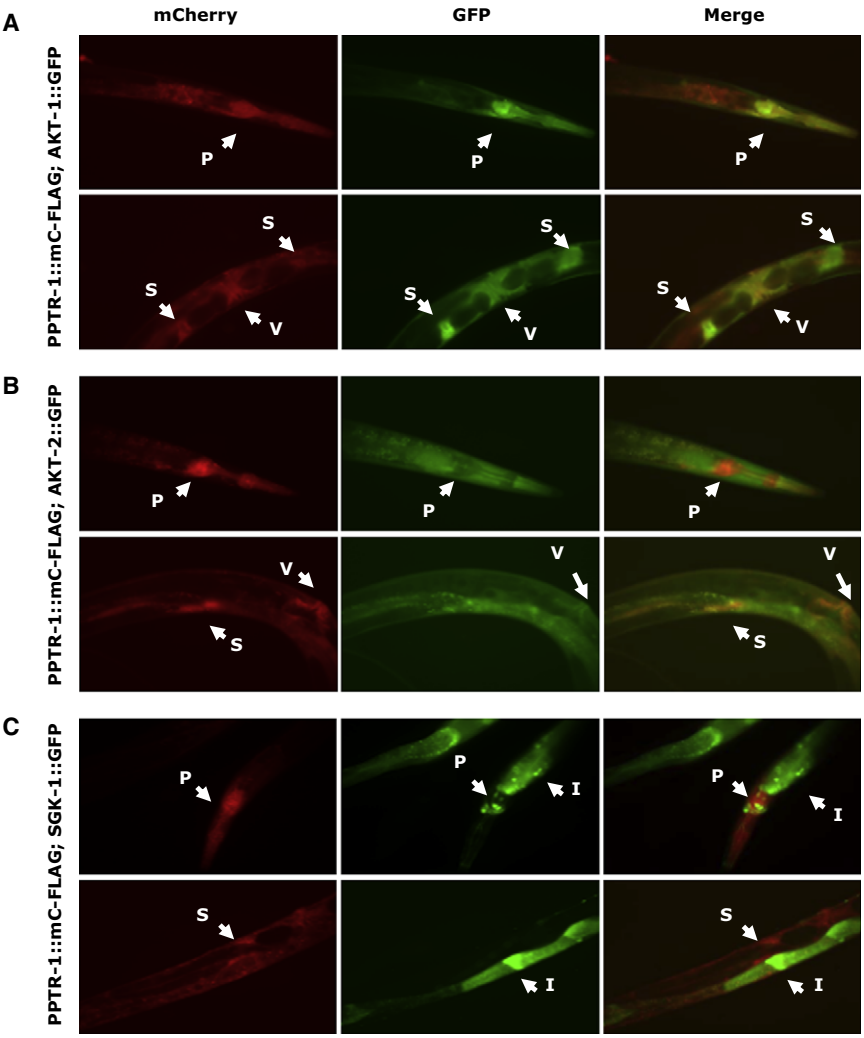

Figure 3. PPTR-1 Colocalizes with AKT-1

akt-1::gfp;pptr-1::mC-flag, *akt-2::gfp;pptr-1::mC-flag*, and *sgk-1::gfp;pptr-1::mC-flag* transgenic worms were mounted and visualized by fluorescence microscopy with Rhodamine (mCherry) and FITC (GFP) filters. PPTR-1 expression is observed mainly in the pharynx, vulva, and spermatheca ([A]–[C], mCherry).

(A) Expression of PPTR-1::mC-FLAG (mCherry) and AKT-1::GFP (GFP) in a *akt-1::gfp; pptr-1::mC-flag* strain. Expression of PPTR-1::mC-FLAG overlaps with AKT-1::GFP (Merge).

(B) PPTR-1::mC-FLAG and AKT-2::GFP colocalize in some tissues in a *akt-2::gfp; pptr-1::mC-flag* strain (Merge).

(C) SGK-1::GFP and PPTR-1::mC-FLAG do not colocalize in *sgk-1::gfp;pptr-1::mC-flag* transgenic worms (Merge).

Arrows indicate the following tissues: p, pharynx; v, vulva; s, spermatheca; i, intestine.

pptr-1::mC-flag and *myo-3::gfp; pptr-1::mcherry-flag* transgenic worms. After immunoprecipitation with either anti-FLAG or anti-GFP antibody, we found that PPTR-1 specifically interacts with AKT-1 and not with MYO-3::GFP (Figure 4A; Experimental Procedures). We also performed co-IP experiments to investigate whether PPTR-1 and AKT-2 interact since we observed partial overlap in expression pattern of these proteins. We find that PPTR-1 does not interact with AKT-2 (Figure S3). Our epistasis analyses show no genetic interaction between *pptr-1* and *sgk-1*. Moreover, we observe no overlap in the expression pattern of these two proteins with confocal microscopy (Movies S1–S8). However, we find that PPTR-1::mC-FLAG and SGK-1::GFP can interact in our co-IP experiments (Figure S3). We do not believe this biochemical interaction to have a measurable functional output and did not pursue it further.

In mammals, Akt is activated by PDK phosphorylation at Thr 308 and PDK-2/TORC-2 protein complex at Ser 473 (Brazil and Hemmings, 2001; Sarbassov et al., 2005). In *C. elegans* AKT-1, these sites correspond to Thr 350 and Ser 517, respectively. We generated affinity-purified phospho-specific antibodies (21st Century BioChemicals, Malboro, MA; Experimental Procedures) against both sites to further investigate the role of PPTR-1 on AKT-1 phosphorylation. After immunoprecipitation with anti-GFP antibody from either *akt-1::gfp* or *akt-1::gfp;pptr-1::mC-flag* strain, we compared the phosphorylation status at these two sites. We find that overexpression of PPTR-1 can dramatically decrease the phosphorylation of the T350 site while having a marginal effect on the Ser 517 site (Figure 4B). As a control experiment, we treated the immunoprecipitated AKT-1::GFP samples with lambda phosphatase and observed loss of the Thr and Ser phosphorylation, showing the specificity of the phospho-AKT antibodies (Figure S4A). Thus, in *C. elegans*, PPTR-1 functions by directly regulating the dephosphorylation of AKT-1 primarily at the Thr 350 (mammalian Thr 308) site.

Mammalian PPTR-1 Homolog Regulates AKT-1 Phosphorylation

Given the evolutionary conservation of the *C. elegans* IIS pathway, we next determined whether this mechanism of AKT-1 dephosphorylation mediated by PPTR-1 is also conserved in mammals. The mammalian B56 family of PP2A regulatory subunits has eight members encoded by five genes that express in different tissues (Eichhorn et al., 2008). We used 3T3-L1 adipocytes to perform these studies since in this system there is a well-characterized insulin signaling pathway that is responsive to changes in insulin levels (Ugi et al., 2004; Watson et al., 2004). We first compared microarray data from the expression profiles of fibroblasts to differentiated 3T3-L1 adipocytes (Powelka et al., 2006) to determine which B56 members were expressed in the adipocytes. We identified two genes, PPP2R5A (B56α) and PPP2R5B (B56β), as the top candidates. We knocked down either one or both these regulatory

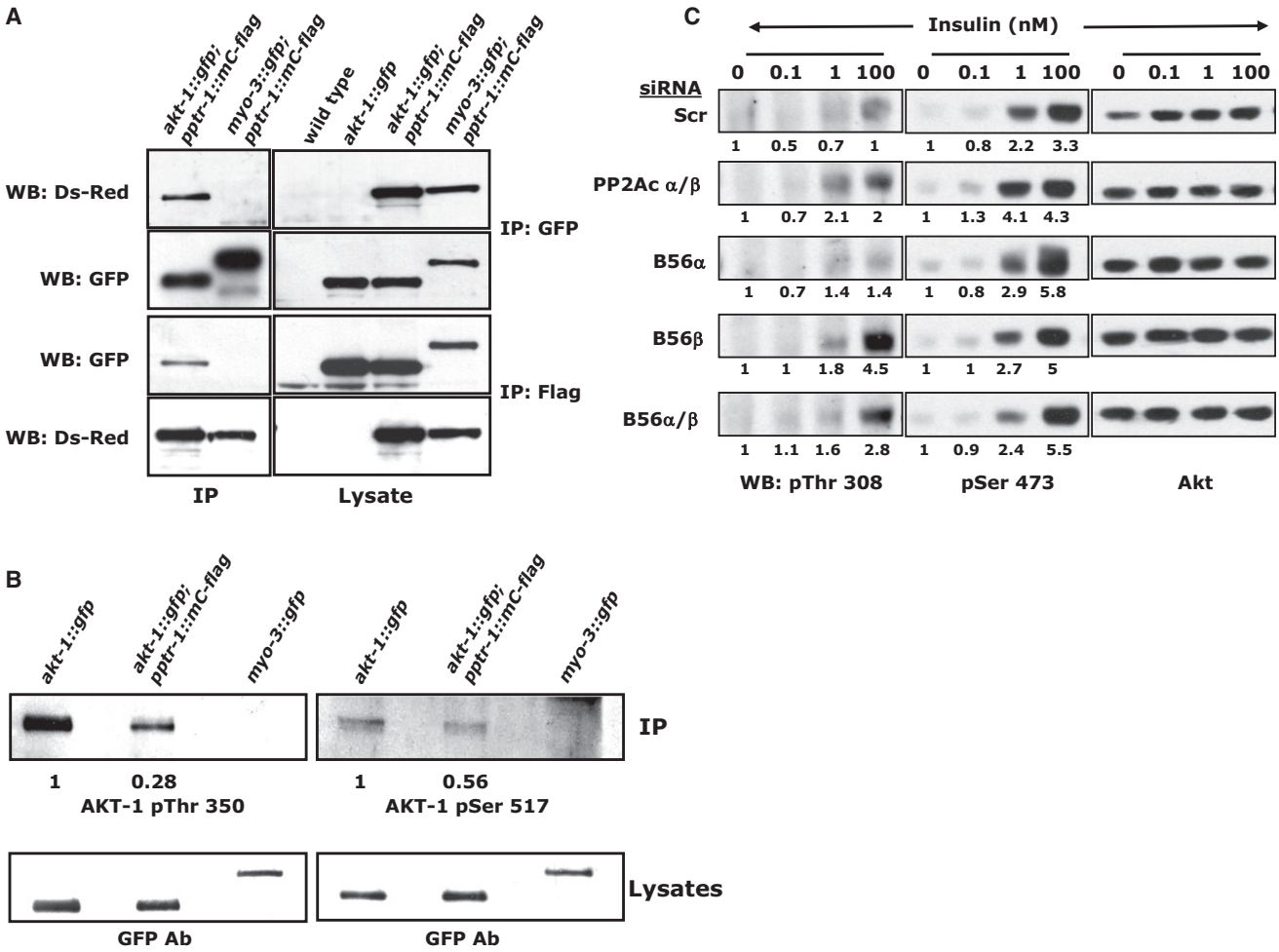

Figure 4. PPTR-1 Interacts with and Modulates AKT-1 Phosphorylation

Data shown are from one representative experiment.

(A) PPTR-1 directly interacts with AKT-1 in *C. elegans*. AKT-1::GFP and MYO-3::GFP were immunoprecipated (IP) with anti-GFP antibody and analyzed by western blotting (WB) with anti-Ds-Red or anti-GFP antibodies. In addition, PPTR-1::mC-FLAG was immunoprecipitated with anti-FLAG antibody and analyzed by WB with anti-Ds-Red or anti-GFP antibodies. Lysates were used for WB analysis.

(B) PPTR-1 overexpression reduces AKT-1 phosphorylation in *C. elegans*. AKT-1::GFP and MYO-3::GFP were immunoprecipitated from *akt-1::gfp, akt-1::gfp;pptr-1::mC-flag* and *myo-3::gfp;pptr-1::mC-flag* followed by western blotting with pThr 350 or pSer 517 antibodies (upper panels). Total lysates were analyzed by western blotting (lower panels). Quantification of changes in AKT-1::GFP phosphorylation upon PPTR-1 overexpression is shown below each lane.

(C) Knockdown of the mammalian B56β regulatory subunit by siRNA in 3T3-L1 adipocytes increases insulin-stimulated AKT phosphorylation at Thr 308. The 3T3-L1 adipocytes were transfected with scrambled (Scr), PP2Acα/β, B56α, B56 β, or B56α/β siRNA. These cells were then treated with increasing concentrations of insulin, and the phosphorylation status of Akt was analyzed by western blotting with pThr 308 (left) and pSer 473 (middle) antibodies. Total Akt antibody was used as a loading control (right). Quantification of fold changes in Akt phosphorylation is shown below each lane.

subunits by designing Smartpool siRNAs (Dharmacon, Lafayette, CO) and verified the silencing by quantitative RT-PCR (Figure S3B). Serum-starved siRNA-treated 3T3-L1 adipocytes were then stimulated with increasing concentrations of insulin. The cells were lysed and the proteins analyzed by Western blotting with mammalian Akt phospho-specific antibodies (Experimental Procedures). Knockdown of B56β results in a dramatic increase in phosphorylation at the Thr 308 site of Akt with relatively less changes in Ser 473 phosphorylation (Figure 4C). However, silencing of B56α had no effect on the phosphorylation status of Akt at either site. We observed that siRNA against both the PP2A catalytic subunits (PP2Acα/β) results in increased phosphorylation at Thr 308 but not at Ser 473. Together, our data suggest that PPTR-1/B56β regulatory subunits function to modulate AKT-1 phosphorylation in a conserved manner across phylogeny.

PPTR-1 Positively Regulates DAF-16 Nuclear Localization

We next determined the consequences of modulating PPTR-1 dosage on the IIS pathway. In *C. elegans*, one of the major targets of AKT-1 is the forkhead transcription factor, DAF-16. Active signaling through the IIS pathway results in the phosphorylation of DAF-16 by AKT-1, AKT-2, and SGK-1, leading to its nuclear

exclusion (Antebi, 2007; Kenyon, 2005; Wolff and Dillin, 2006). However, under low signaling conditions, DAF-16 translocates into the nucleus, where it can directly bind and activate/repress the transcription of target genes involved in dauer formation, life span, stress resistance, and fat storage (Oh et al., 2006). We asked whether *pptr-1* regulates IIS pathway-specific phenotypes by modulating DAF-16 function. Since we observed reduced phosphorylation of AKT-1 upon overexpression of PPTR-1, we first looked at the effect of PPTR-1 overexpression on DAF-16 nuclear localization (Henderson and Johnson, 2001; Lee et al., 2001; Lin et al., 2001). We generated a *daf-16::gfp;pptr-1::mC-flag* strain and then compared the DAF-16 nuclear localization in these worms with a *daf-16*::*gfp* strain (Figure 5A and Figure S5A). We categorized DAF-16::GFP localization as completely cytosolic, mostly cytosolic, mostly nuclear, or completely nuclear. We find that DAF-16::GFP nuclear localization is enhanced when PPTR-1 is overexpressed (Figure 5A and Figure S5A). To determine the specificity of this response, we used *mCherry* RNAi to effectively knock down *mCherry* expression in *pptr-1::mC-flag*, thereby reducing the expression of *pptr-1* transgene (data not shown). Our results show that the enhanced nuclear localization upon PPTR-1 overexpression is suppressed when *pptr-1::mC-flag;daf-16*::*gfp* worms are grown on *mCherry* RNAi (Figure 5A and Figure S5A) and that *mCherry* RNAi has little effect on DAF-16 localization in *daf-16*::*gfp* worms. These experiments suggest that increased dosage of *pptr-1* affects DAF-16 nuclear localization. Consistent with its role in the *C. elegans* IIS pathway, we find that overexpression of *pptr-1* significantly increases the life span of wild-type worms but does not further enhance the life span *daf-2(e1370)* worms (Figure 5B and Table S3B; mean life span of the wild-type is 23.9 ± 0.3 days, *pptr-1::mC-flag* is 30.1 ± 0.5 days, $p < 0.0001$, and the *unc-119(+); unc-119(ed3)* control strain is 22.6 ± 0.3 days).

As a corollary to this experiment, we next looked at the effect of *pptr-1*RNAi on DAF-16 nuclear localization. For this, we generated a strain with a *daf-2(e1370);daf-16::gfp* strain. At the permissive temperature of 15°C, DAF-16::GFP is excluded from the nucleus in the *daf-2(e1370);daf-16::gfp* strain. However, at the nonpermissive temperature of 25°C, progressive nuclear localization of DAF-16::GFP is observed. We grew *daf-2(e1370); daf-16::gfp* worms on vector, *pptr-1*, or *daf-18* RNAi and measured the extent of nuclear localization at 25°C. We find that *pptr*-1 RNAi significantly reduced DAF-16 nuclear localization, similar to the effect of *daf-18* RNAi (Figure 5C and Figure S5B). Together, these experiments suggest that changes in PPTR-1 levels affect the activity of AKT-1 and, as a result, modulate DAF-16 subcellular localization.

PPTR-1 Positively Regulates DAF-16 Target Genes

DAF-16 regulates the transcription of many downstream genes such as *sod-3*, *hsp-12.6*, *sip-1*, and *mtl-1* (Furuyama et al., 2000; Lee et al., 2003; McElwee et al., 2003; Murphy et al., 2003; Oh et al., 2006). We next tested the effects of *pptr-1* RNAi on these DAF-16 transcriptional targets. We first tested *sod-3*, which has been shown to be a direct target of DAF-16 by chromatin immunoprecipitation (Oh et al., 2006), and its expression changes in response to modulation of the IIS pathway (Furuyama et al., 2000; Libina et al., 2003; Murphy et al., 2003). We grew a *daf-2(e1370);Psod-3::gfp(muIs84)* strain on vector, *daf-18*, or *pptr-1* RNAi to look at the effect on GFP expression. Similar to worms grown on *daf-18* RNAi, *pptr-1* RNAi reduces expression of GFP (Figure 5D and Figure S5C). Therefore, modulation in the levels of *pptr-1* can affect the expression of direct DAF-16 target genes.

We further analyzed the expression of known DAF-16 target genes by quantitative RT-PCR in a *daf-2(e1370)* mutant background. As a control, we analyzed whether each of these target genes expressed in a *daf-16*-dependent manner as previously reported (McElwee et al., 2003; Murphy et al., 2003; Oh et al., 2006). As shown in Figure 5E and Figure S5D, *daf-16* RNAi dramatically suppressed the expression levels of these genes. Next, we tested the effects of either *pptr-1* or *daf-18* RNAi on the expression of these genes. We found that *pptr-1* RNAi also suppressed the expression of these genes to a level similar to *daf-18* RNAi. Taken together, our data suggest that PPTR-1 positively regulates DAF-16 nuclear localization and thereby its activity.

DISCUSSION

In a directed RNAi screen for Ser/Thr phosphatases in the *C. elegans* IIS pathway, we identified *pptr-1*, a B56 regulatory subunit of the PP2A holoenzyme. PP2A itself is a ubiquitously expressed phosphatase that is involved in multiple cellular processes including regulation of insulin signaling by direct dephosphorylation of Akt (Andjelkovic et al., 1996; Resjo et al., 2002; Ugi et al., 2004). Substrate specificity of PP2A is achieved by its association with distinct regulatory subunits. Our studies provide a mechanistic insight into how the *C. elegans* PP2A regulatory subunit PPTR-1 modulates insulin signaling by specifically regulating AKT-1 phosphorylation and activity in the context of a whole organism.

In our model (Figure 5F), PPTR-1 acts to negatively regulate signals transduced through the IIS pathway, ultimately controlling the activity of the FOXO transcription factor DAF-16. Under low signaling conditions, DAF-16 is able to translocate to the nucleus and transactivate or repress its downstream targets. It is well established that AKT modulates DAF-16 subcellular localization. Thus, the activity of AKT-1, as governed by its phosphorylation status, directly translates into the activity of DAF-16. In this study, we show that PPTR-1 directly interacts with AKT-1 and regulates its activity by modulating its phosphorylation, predominantly at the Thr 350 site. Less active AKT-1 results in increased DAF-16 nuclear localization. Indeed, DAF-16 is found to be more nuclear throughout the worm when PPTR-1 is overexpressed. As a corollary, knockdown of *pptr-1* by RNAi results in less nuclear DAF-16 as well as reduced expression of DAF-16 target genes such as *sod-3*, *hsp-12.6*, *mtl-1*, and *sip-1*. These genes are known to play a combinatorial role in adaptation to various stresses, leading to enhanced dauer formation and increased life span. Consistent with the decreased levels of these important genes, *pptr-1* RNAi results in a significant decrease in the dauer formation, life span, and thermotolerance of *daf-2(e1370)* mutants. In addition, *pptr-1* also regulates other DAF-16-dependent outputs of the IIS pathway, such as fat storage. Thus, we find that normal levels of *pptr-1* are important under low insulin signaling conditions.

A

Strains	RNAi	Completely Cytoplasmic (%)	Mostly Cytoplasmic (%)	Mostly Nuclear (%)	Completely Nuclear (%)	(n)
pptr-1::mC-flag; daf-16::gfp	vector	34.5	22.9	29.6	12.9	77
	mCherry	79.5	18.6	1.95	0	96
daf-16::gfp	vector	50.0	42.5	5.0	2.5	40
	mCherry	55.3	29.8	14.9	0	47

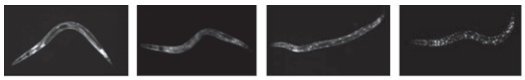

C

Strain	RNAi	Completely Cytoplasmic (%)	Mostly cytoplasmic (%)	Mostly Nuclear (%)	Completely Nuclear (%)	(n)
daf-2(e1370); daf-16::gfp	vector	4.5	40.9	50.0	4.5	22
	daf-18	63.6	45.4	4.5	0	25
	pptr-1	50.0	45.4	4.5	0	22

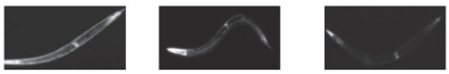

D

Strain	RNAi	High (%)	Medium (%)	Low (%)	(n)
daf-2(e1370); sod-3::gfp	vector	36.6	46.6	16.6	30
	daf-18	10.0	50.0	40.0	30
	pptr-1	6.6	43.3	50.0	30

E

Strain	RNAi	Transcripts determined by Q-PCR (% of vector RNAi)			
		sod-3	*hsp-12.6*	*sip-1*	*mtl-1*
daf-2(e1370)	*daf-16*	7.8	10.8	24.7	0.7
	daf-18	46.8	35.2	84.1	17.8
	pptr-1	45.2	52.2	86.7	32.0

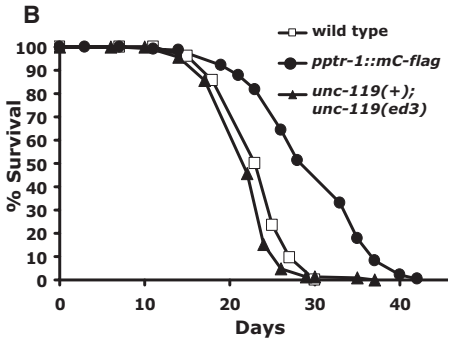

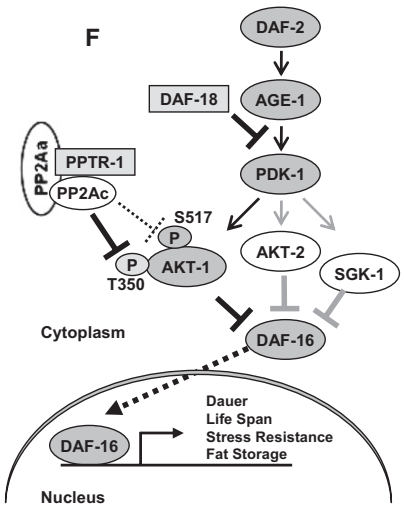

Figure 5. PPTR-1 Regulates DAF-16 Localization and Activity

Data shown are from one representative experiment.

(A) Overexpression of PPTR-1 promotes DAF-16 nuclear translocation. On vector RNAi, DAF-16 is more enriched in the nucleus in a *pptr-1::mC-flag;daf-16::gfp* strain, compared to a *daf-16::gfp* strain. This effect is specific to the functional transgene, as knockdown of *pptr-1::mC-flag* with *mCherry* RNAi decreases the extent of nuclear DAF-16.

(B) Overexpression of PPTR-1 significantly increases the life span of wild-type worms. Mean life span [days ± SD (n)] of wild-type worms is 23.9 ± 0.3 days (n = 154); of *pptr-1::mC-flag* is 30.1 ± 0.5 days (n = 202), $p < 0.0001$; and of the *unc-119(+); unc-119(ed3)* control strain is 22.6 ± 0.3 days (n = 145).

(C) In a *daf-2(e1370);daf-16::gfp* strain, DAF-16 is enriched in the nucleus on vector RNAi, whereas on *pptr-1* RNAi as well as *daf-18* RNAi, DAf-16 is mostly cytosolic.

(D) *pptr-1* RNAi affects DAF-16 transcriptional activity. *sod-3* is one of the direct targets of DAF-16. *pptr*-1 RNAi reduces *Psod-3::*GFP expression in a *daf-2(e1370);Psod-3::gfp(muls84)* strain, similar to *daf-18* RNAi.

(E) Transcript abundance of known DAF-16 target genes decrease when *daf-2(e1370)* worms are grown on *pptr-1* RNAi, similar to *daf-18* RNAi, as detected by real-time PCR.

(F) Proposed model illustrating the role of PPTR-1 in the insulin/IGF-1 signaling pathway. Signals from DAF-2 are processed by a PI3-kinase pathway that leads to the phosphorylation and activation of downstream serine/threonine kinases such as PDK-1, AKT-1, AKT-2, and SGK-1. PPTR-1, the PP2A holoenzyme regulatory subunit, regulates the dephosphorylation and activation status of AKT-1 at T350. This in turn affects the nuclear translocation of DAF-16 and the expression of genes involved in life span, dauer formation, stress resistance, and fat storage.

However, *pptr-1* RNAi does not affect IIS pathway-associated phenotypes in wild-type worms. There could be several reasons for this observation. First, under normal signaling conditions, AKT-1, AKT-2, and SGK-1 are active and negatively regulate DAF-16. Therefore, changes in the AKT-1 activity alone brought about by *pptr-1* RNAi may not have a significant effect on DAF-16-dependent phenotypes. Second, PPTR-1 itself may be negatively regulated by the IIS pathway, leading to increased AKT-1 phosphorylation. Along similar lines, in mammals, insulin signaling can downregulate the expression and activity of the PP2A catalytic subunit (Hojlund et al., 2002; Srinivasan and Begum, 1994; Ugi et al., 2004). Thus, under normal conditions, further downregulation of *pptr-1* by RNAi may have no effect. We speculate that in *C elegans*, in response to changing environmental cues, PPTR-1 helps to downregulate the insulin signaling pathway to promote DAF-16 activity, enabling the worm to either enter diapause or enhance its tolerance to stress as adults.

In mammals, Akt controls a myriad of secondary signaling cascades that regulate glucose transport, protein synthesis,

genomic stability, cell survival, and gene expression (Toker and Yoeli-Lerner, 2006). Previous studies have implicated roles for PP2A and PHLPP phosphatases in the negative regulation of Akt (Kuo et al., 2008). The PP2A inhibitor Okadaic acid can increase Akt phosphorylation predominantly at Thr 308 and enhance glucose transport in adipocytes (Rondinone et al., 1999). Consistent with this, our results show that siRNA knockdown of the PP2A catalytic subunit and, more importantly, the B56β regulatory subunit results in enhanced Akt phosphorylation at Thr 308 in 3T3-L1 adipocytes. Thus, our study points at the remarkable functional conservation of the B56/PPTR-1 regulatory subunit of PP2A in regulating AKT phosphorylation between *C. elegans* and higher mammals. In worms, we also see a modest effect on Ser 517 (equivalent to mammalian Ser 473) phosphorylation by PPTR-1 overexpression. However, we do not observe a difference in Ser 473 phosphorylation in adipocytes. This difference may be explained by the fact that in worms, we are determining the phosphorylation of AKT-1 in the context of a whole organism. Additionally, in mammals, phosphorylation state of one Akt site may influence the status of the other (Gao et al., 2005; Toker and Newton, 2000). We do not see a role for the PP2A B55 subunit (*sur-6*) in the *C. elegans* IIS pathway. However, a recent report using cell culture has implicated the mammalian B55 in the regulation of AKT (Kuo et al., 2008).

Dysregulation of Akt has been implicated in diseases such as cancer and diabetes (Rondinone et al., 1999; Sasaoka et al., 2006; Smith et al., 1999; Zdychova and Komers, 2005). In fact, the onset of diabetes is often associated with changes in Akt phosphorylation (Zdychova and Komers, 2005). In several cancer models, loss-of-function mutations in the PTEN results in hyperphosphorylated and activated Akt (Groszer et al., 2001; Hakem and Mak, 2001; Stiles et al., 2002; Testa and Bellacosa, 2001) Our studies show that, like PTEN, PPTR-1 acts to negatively regulate the insulin/IGF-1 signaling. Given the important role of PPTR-1/B56 in modulating Akt activity, this protein may be a potential therapeutic target for the treatment of diabetes as well as cancer.

EXPERIMENTAL PROCEDURES

Strains

All strains were maintained at 15°C via standard *C. elegans* techniques (Stiernagle, 2006). Double mutants were made by standard genetic methods, while transgenic worms were made by microparticle bombardment as described in the Supplemental Experimental Procedures. For all RNAi assays, the worms were grown for at least two full generations on the RNAi bacteria. Preparation of RNAi plates is described in the Supplemental Experimental Procedures.

C. elegans Assays

C. elegans assays were modified from previously published methods (Henderson and Johnson, 2001; Kimura et al., 1997; Libina et al., 2003; Oh et al., 2006; Oh et al., 2005). For detailed description of these assays, see the Supplemental Experimental Procedures.

C. elegans Immunoprecipitation and Western Blotting

Transgenic worms were grown in three 100 mm plates seeded with OP50 bacteria at 20°C. Worms were harvested by washing with M9 buffer and pellet collected by centrifugation. The pellet was resuspended in 250 μl lysis buffer (20 mM Tris-Cl, 137 mM NaCl, 10% glycerol, 1% Triton X-100, 25 mM β-glycerophosphate, Protease inhibitor cocktail [Roche Biochemicals, Indianapolis, IN] [pH 7.4]). The worms were sonicated with Bioruptor (Diagenode, Sparta, NJ) using maximum power output (1 min sonication, 2 min off—repeated ten times). The lysate was cleared by centrifugation, and protein content was estimated by the Bradford method. Lysate equivalent to 1.5 mg total protein was precleared with 50 μl of protein-G agarose beads, fast flow (Upstate, Billerica, MA) and then immunoprecipitated overnight at 4°C with either anti-GFP monoclonal antibody (Sigma, St. Louis, MO) or anti-FLAG M2 gel (Sigma). The following morning, 50 μl protein-G agarose beads, fast flow were added to the GFP immunoprecipitation (IP) to capture the immune complex. The agarose beads were then washed five times with lysis buffer. After this step, the beads were boiled in Laemelli's buffer.

For Western blot analysis, immunoprecipitated protein samples was resolved on a 10% SDS-PAGE and transferred to nitrocellulose membranes. Membranes were blocked in TBST (Tris-Buffered Saline containing 0.05% Tween 20 [ph 7.4]) containing 5% nonfat milk at room temperature for 1 hr. Membranes were then washed with TBST and incubated overnight with 1:1000 dilutions of antibodies in TBST containing 5% nonfat milk at 4°C. Membranes were washed three times with TBST and then incubated with TBST containing 5% nonfat milk containing a 1:10,000 dilution of the secondary antibody. Antibodies used for western were the following:

Living Color DsRed antibody (Clontech, Mountain View, CA; catalog number 632496)
Living Color Rabbit polyclonal GFP antibody (BD Biosciences, San Jose, CA; catalog number 632460)
Monoclonal mAb 3e6 GFP antibody (Invitrogen, Carlsbad, CA; catalog number A11120)
Anti-FLAG M2 Affinity Gel (Sigma; catalog number A2220).

C. elegans Phospho-AKT Western Blotting

Transgenic worms were grown at 20°C in 3–4 large (100 mm) plates seeded with OP50. Worms were collected by washing with 1× PBS and the pellet was then immediately frozen in dry ice. Around 500 μl lysis buffer, supplemented by Sigma Phosphatase inhibitor cocktails I and II (50×) and Protease inhibitor cocktail (Roche Biochemicals) was added to the pellet and sonicated with a Misonix (3000) sonicator (Misonix, Farmingdale, NY; power output set at 4, three pulses of 10 s each with 1 min interval between pulses). The lysates were clarified by centrifugation at 13,000 rpm for 10 min at 4°C, and the protein content was estimated by Quick Bradford (Pierce). About 3.5 μg of anti-GFP monoclonal antibody (3E6, Invitrogen USA) was used for each IP from lysates containing 1.7 mg protein in a volume of 1 ml. IPs were performed overnight at 4°C and antibody-protein complexes were captured with 50 μl of protein-G agarose beads, fast flow (Upstate) for 2 hr at 4°C. The pellets were washed three times with lysis buffer supplemented by protease and phosphatase inhibitors and boiled in Laemelli's buffer. The IP samples were then resolved on a 10% SDS-PAGE, western blotted, and analyzed with phospho-specific antibodies (Supplemental Experimental Procedures).

Mammalian Cell Culture and Phospho-Akt Western Blotting

3T3-L1 adipocytes were cultured and differentiated as previously described (Tesz et al., 2007). For siRNA transfections, cells from 4 days after induction of adipocyte differentiation were used as previously described (Tang et al., 2006). Cells were stimulated with increasing concentrations of insulin, and isolated proteins were analyzed by western blotting. The detailed procedure is described in the Supplemental Experimental Procedures.

RNA Isolation and Real-Time PCR

Total RNA was isolated with Trizol (Invitrogen), and real-time PCR was performed according to the manufacturer's instructions (Applied Biosystems, Foster City, CA) as detailed in the Supplemental Experimental Procedures.

SUPPLEMENTAL DATA

Supplemental Data include Supplemental Experimental Procedures, five figures, seven tables, and eight movies and can be found with this article online at http://www.cell.com/supplemental/S0092-8674(09)00073-7.

ACKNOWLEDGMENTS

We are grateful to Eun-soo Kwon, Kelvin Yen, Craig Mello, and Marian Walhout for advice and critical comments on the manuscript, Paul Furcinitti of the UMass Medical School Digital Light Microscopy Core Facility for help with the confocal microscopy, Nina Bhabhalia for technical support, and Sandhya Pande for help with the phospho-westerns. We thank Marian Walhout, Gary Ruvkun, Maren Hertweck, and Ralf Baumeister for plasmids and strains. Some of the strains were kindly provided by Theresa Stiernagle at the *Caenorhabditis* Genetics Center, which is funded by the National Institutes of Health National Center for Research Resources. H.A.T. is a William Randolph Hearst Young Investigator. This project was funded in part by the National Institute of Aging (AG025891), the Glenn Foundation, and an endowment from the William Randolph Hearst Foundation.

Received: October 8, 2008
Revised: December 18, 2008
Accepted: January 16, 2009
Published online: February 26, 2009

REFERENCES

Andjelkovic, M., Jakubowicz, T., Cron, P., Ming, X.F., Han, J.W., and Hemmings, B.A. (1996). Activation and phosphorylation of a pleckstrin homology domain containing protein kinase (RAC-PK/PKB) promoted by serum and protein phosphatase inhibitors. Proc. Natl. Acad. Sci. USA *93*, 5699–5704.

Antebi, A. (2007). Genetics of aging in *Caenorhabditis elegans*. PLoS Genet. *3*, 1565–1571.

Ashrafi, K., Chang, F.Y., Watts, J.L., Fraser, A.G., Kamath, R.S., Ahringer, J., and Ruvkun, G. (2003). Genome-wide RNAi analysis of *Caenorhabditis elegans* fat regulatory genes. Nature *421*, 268–272.

Barbieri, M., Bonafe, M., Franceschi, C., and Paolisso, G. (2003). Insulin/IGF-I-signaling pathway: an evolutionarily conserved mechanism of longevity from yeast to humans. Am. J. Physiol. Endocrinol. Metab. *285*, E1064–E1071.

Brazil, D.P., and Hemmings, B.A. (2001). Ten years of protein kinase B signalling: a hard Akt to follow. Trends Biochem. Sci. *26*, 657–664.

Brunet, A., Bonni, A., Zigmond, M.J., Lin, M.Z., Juo, P., Hu, L.S., Anderson, M.J., Arden, K.C., Blenis, J., and Greenberg, M.E. (1999). Akt promotes cell survival by phosphorylating and inhibiting a Forkhead transcription factor. Cell *96*, 857–868.

Brunet, A., Park, J., Tran, H., Hu, L.S., Hemmings, B.A., and Greenberg, M.E. (2001). Protein kinase SGK mediates survival signals by phosphorylating the forkhead transcription factor FKHRL1 (FOXO3a). Mol. Cell. Biol. *21*, 952–965.

da Graca, L.S., Zimmerman, K.K., Mitchell, M.C., Kozhan-Gorodetska, M., Sekiewicz, K., Morales, Y., and Patterson, G.I. (2004). DAF-5 is a Ski oncoprotein homolog that functions in a neuronal TGF beta pathway to regulate *C. elegans* dauer development. Development *131*, 435–446.

Dorman, J.B., Albinder, B., Shroyer, T., and Kenyon, C. (1995). The *age-1* and *daf-2* genes function in a common pathway to control the lifespan of *Caenorhabditis elegans*. Genetics *141*, 1399–1406.

Eichhorn, P.J., Creyghton, M.P., and Bernards, R. (2008). Protein phosphatase 2A regulatory subunits and cancer. Biochim. Biophys. Acta *1795*, 1–15.

Fire, A., Xu, S., Montgomery, M.K., Kostas, S.A., Driver, S.E., and Mello, C.C. (1998). Potent and specific genetic interference by double-stranded RNA in *Caenorhabditis elegans*. Nature *391*, 806–811.

Furuyama, T., Nakazawa, T., Nakano, I., and Mori, N. (2000). Identification of the differential distribution patterns of mRNAs and consensus binding sequences for mouse DAF-16 homologues. Biochem. J. *349*, 629–634.

Gao, T., Furnari, F., and Newton, A.C. (2005). PHLPP: a phosphatase that directly dephosphorylates Akt, promotes apoptosis, and suppresses tumor growth. Mol. Cell *18*, 13–24.

Gems, D., Sutton, A.J., Sundermeyer, M.L., Albert, P.S., King, K.V., Edgley, M.L., Larsen, P.L., and Riddle, D.L. (1998). Two pleiotropic classes of *daf-2* mutation affect larval arrest, adult behavior, reproduction and longevity in Caenorhabditis elegans. Genetics *150*, 129–155.

Gil, E.B., Malone Link, E., Liu, L.X., Johnson, C.D., and Lees, J.A. (1999). Regulation of the insulin-like developmental pathway of *Caenorhabditis elegans* by a homolog of the PTEN tumor suppressor gene. Proc. Natl. Acad. Sci. USA *96*, 2925–2930.

Groszer, M., Erickson, R., Scripture-Adams, D.D., Lesche, R., Trumpp, A., Zack, J.A., Kornblum, H.I., Liu, X., and Wu, H. (2001). Negative regulation of neural stem/progenitor cell proliferation by the Pten tumor suppressor gene in vivo. Science *294*, 2186–2189.

Gunther, C.V., Georgi, L.L., and Riddle, D.L. (2000). A *Caenorhabditis elegans* type I TGF beta receptor can function in the absence of type II kinase to promote larval development. Development *127*, 3337–3347.

Hakem, R., and Mak, T.W. (2001). Animal models of tumor-suppressor genes. Annu. Rev. Genet. *35*, 209–241.

Henderson, S.T., and Johnson, T.E. (2001). *daf-16* integrates developmental and environmental inputs to mediate aging in the nematode *Caenorhabditis elegans*. Curr. Biol. *11*, 1975–1980.

Hertweck, M., Gobel, C., and Baumeister, R. (2004). *C. elegans* SGK-1 is the critical component in the Akt/PKB kinase complex to control stress response and life span. Dev. Cell *6*, 577–588.

Hojlund, K., Poulsen, M., Staehr, P., Brusgaard, K., and Beck-Nielsen, H. (2002). Effect of insulin on protein phosphatase 2A expression in muscle in type 2 diabetes. Eur. J. Clin. Invest. *32*, 918–923.

Honda, Y., and Honda, S. (1999). The *daf-2* gene network for longevity regulates oxidative stress resistance and Mn-superoxide dismutase gene expression in *Caenorhabditis elegans*. FASEB J. *13*, 1385–1393.

Inoue, T., and Thomas, J.H. (2000). Targets of TGF-beta signaling in *Caenorhabditis elegans* dauer formation. Dev. Biol. *217*, 192–204.

Janssens, V., Longin, S., and Goris, J. (2008). PP2A holoenzyme assembly: in cauda venenum (the sting is in the tail). Trends Biochem. Sci. *33*, 113–121.

Jensen, V.L., Albert, P.S., and Riddle, D.L. (2007). *Caenorhabditis elegans* SDF-9 enhances insulin/insulin-like signaling through interaction with DAF-2. Genetics *177*, 661–666.

Kamath, R.S., Fraser, A.G., Dong, Y., Poulin, G., Durbin, R., Gotta, M., Kanapin, A., Le Bot, N., Moreno, S., Sohrmann, M., et al. (2003). Systematic functional analysis of the *Caenorhabditis elegans* genome using RNAi. Nature *421*, 231–237.

Kenyon, C. (2005). The plasticity of aging: insights from long-lived mutants. Cell *120*, 449–460.

Kenyon, C., Chang, J., Gensch, E., Rudner, A., and Tabtiang, R. (1993). A *C. elegans* mutant that lives twice as long as wild type. Nature *366*, 461–464.

Kimble, J., Edgar, L., and Hirsh, D. (1984). Specification of male development in *Caenorhabditis elegans*: the fem genes. Dev. Biol. *105*, 234–239.

Kimura, K.D., Tissenbaum, H.A., Liu, Y., and Ruvkun, G. (1997). *daf-2*, an insulin receptor-like gene that regulates longevity and diapause in *Caenorhabditis elegans*. Science *277*, 942–946.

Kuo, Y.C., Huang, K.Y., Yang, C.H., Yang, Y.S., Lee, W.Y., and Chiang, C.W. (2008). Regulation of phosphorylation of Thr-308 of Akt, cell proliferation, and survival by the B55alpha regulatory subunit targeting of the protein phosphatase 2A holoenzyme to Akt. J. Biol. Chem. *283*, 1882–1892.

Larsen, P.L., Albert, P.S., and Riddle, D.L. (1995). Genes that regulate both development and longevity in *Caenorhabditis elegans*. Genetics *139*, 1567–1583.

Lee, R.Y., Hench, J., and Ruvkun, G. (2001). Regulation of *C. elegans* DAF-16 and its human ortholog FKHRL1 by the *daf-2* insulin-like signaling pathway. Curr. Biol. *11*, 1950–1957.

Lee, S.S., Kennedy, S., Tolonen, A.C., and Ruvkun, G. (2003). DAF-16 target genes that control *C. elegans* life-span and metabolism. Science *300*, 644–647.

Libina, N., Berman, J.R., and Kenyon, C. (2003). Tissue-specific activities of *C. elegans* DAF-16 in the regulation of lifespan. Cell *115*, 489–502.

Lin, K., Dorman, J.B., Rodan, A., and Kenyon, C. (1997). *daf-16*: An HNF-3/forkhead family member that can function to double the life-span of *Caenorhabditis elegans*. Science *278*, 1319–1322.

Lin, K., Hsin, H., Libina, N., and Kenyon, C. (2001). Regulation of the *Caenorhabditis elegans* longevity protein DAF-16 by insulin/IGF-1 and germline signaling. Nat. Genet. *28*, 139–145.

Lithgow, G.J., and Walker, G.A. (2002). Stress resistance as a determinate of *C. elegans* lifespan. Mech. Ageing Dev. *123*, 765–771.

Lithgow, G.J., White, T.M., Melov, S., and Johnson, T.E. (1995). Thermotolerance and extended life-span conferred by single-gene mutations and induced by thermal stress. Proc. Natl. Acad. Sci. USA *92*, 7540–7544.

McElwee, J., Bubb, K., and Thomas, J.H. (2003). Transcriptional outputs of the *Caenorhabditis elegans* forkhead protein DAF-16. Aging Cell *2*, 111–121.

Mihaylova, V.T., Borland, C.Z., Manjarrez, L., Stern, M.J., and Sun, H. (1999). The PTEN tumor suppressor homolog in *Caenorhabditis elegans* regulates longevity and dauer formation in an insulin receptor-like signaling pathway. Proc. Natl. Acad. Sci. USA *96*, 7427–7432.

Morris, J.Z., Tissenbaum, H.A., and Ruvkun, G. (1996). A phosphatidylinositol-3-OH kinase family member regulating longevity and diapause in *Caenorhabditis elegans*. Nature *382*, 536–539.

Mukhopadhyay, A., Oh, S.W., and Tissenbaum, H.A. (2006). Worming pathways to and from DAF-16/FOXO. Exp. Gerontol. *41*, 928–934.

Munoz, M.J., and Riddle, D.L. (2003). Positive selection of *Caenorhabditis elegans* mutants with increased stress resistance and longevity. Genetics *163*, 171–180.

Murphy, C.T., McCarroll, S.A., Bargmann, C.I., Fraser, A., Kamath, R.S., Ahringer, J., Li, H., and Kenyon, C. (2003). Genes that act downstream of DAF-16 to influence the lifespan of *Caenorhabditis elegans*. Nature *424*, 277–283.

Ogg, S., and Ruvkun, G. (1998). The *C. elegans* PTEN homolog, DAF-18, acts in the insulin receptor-like metabolic signaling pathway. Mol. Cell *2*, 887–893.

Ogg, S., Paradis, S., Gottlieb, S., Patterson, G.I., Lee, L., Tissenbaum, H.A., and Ruvkun, G. (1997). The Fork head transcription factor DAF-16 transduces insulin-like metabolic and longevity signals in *C. elegans*. Nature *389*, 994–999.

Oh, S.W., Mukhopadhyay, A., Svrzikapa, N., Jiang, F., Davis, R.J., and Tissenbaum, H.A. (2005). JNK regulates lifespan in *Caenorhabditis elegans* by modulating nuclear translocation of forkhead transcription factor/DAF-16. Proc. Natl. Acad. Sci. USA *102*, 4494–4499.

Oh, S.W., Mukhopadhyay, A., Dixit, B.L., Raha, T., Green, M.R., and Tissenbaum, H.A. (2006). Identification of direct DAF-16 targets controlling longevity, metabolism and diapause by chromatin immunoprecipitation. Nat. Genet. *38*, 251–257.

Paradis, S., Ailion, M., Toker, A., Thomas, J.H., and Ruvkun, G. (1999). A PDK1 homolog is necessary and sufficient to transduce AGE-1 PI3 kinase signals that regulate diapause in *Caenorhabditis elegans*. Genes Dev. *13*, 1438–1452.

Paradis, S., and Ruvkun, G. (1998). *Caenorhabditis elegans* Akt/PKB transduces insulin receptor-like signals from AGE-1 PI3 kinase to the DAF-16 transcription factor. Genes Dev. *12*, 2488–2498.

Patterson, G.I., Koweek, A., Wong, A., Liu, Y., and Ruvkun, G. (1997). The DAF-3 Smad protein antagonizes TGF-beta-related receptor signaling in the *Caenorhabditis elegans* dauer pathway. Genes Dev. *11*, 2679–2690.

Patterson, G.I., and Padgett, R.W. (2000). TGF beta-related pathways. Roles in *Caenorhabditis elegans* development. Trends Genet. *16*, 27–33.

Pilgrim, D., McGregor, A., Jackle, P., Johnson, T., and Hansen, D. (1995). The *C. elegans* sex-determining gene *fem-2* encodes a putative protein phosphatase. Mol. Biol. Cell *6*, 1159–1171.

Powelka, A.M., Seth, A., Virbasius, J.V., Kiskinis, E., Nicoloro, S.M., Guilherme, A., Tang, X., Straubhaar, J., Cherniack, A.D., Parker, M.G., and Czech, M.P. (2006). Suppression of oxidative metabolism and mitochondrial biogenesis by the transcriptional corepressor RIP140 in mouse adipocytes. J. Clin. Invest. *116*, 125–136.

Reboul, J., Vaglio, P., Rual, J.F., Lamesch, P., Martinez, M., Armstrong, C.M., Li, S., Jacotot, L., Bertin, N., Janky, R., et al. (2003). *C. elegans* ORFeome version 1.1: experimental verification of the genome annotation and resource for proteome-scale protein expression. Nat. Genet. *34*, 35–41.

Ren, P., Lim, C., Johnsen, R., Albert, P.S., Pilgrim, D., and Riddle, D.L. (1996). Control of *C. elegans* larval development by neuronal expression of a TGF-β homologue. Science *274*, 1389–1391.

Resjo, S., Goransson, O., Harndahl, L., Zolnierowicz, S., Manganiello, V., and Degerman, E. (2002). Protein phosphatase 2A is the main phosphatase involved in the regulation of protein kinase B in rat adipocytes. Cell. Signal. *14*, 231–238.

Riddle, D., Blumenthal, T., Meyer, B., and Priess, J. (1997). *C. Elegans* II (Cold Spring Harbor: Cold Spring Harbor Press).

Riddle, D.L., Swanson, M.M., and Albert, P.S. (1981). Interacting genes in nematode dauer larva formation. Nature *290*, 668–671.

Rondinone, C.M., Carvalho, E., Wesslau, C., and Smith, U.P. (1999). Impaired glucose transport and protein kinase B activation by insulin, but not okadaic acid, in adipocytes from subjects with Type II diabetes mellitus. Diabetologia *42*, 819–825.

Rouault, J.P., Kuwabara, P.E., Sinilnikova, O.M., Duret, L., Thierry-Mieg, D., and Billaud, M. (1999). Regulation of dauer larva development in *Caenorhabditis elegans* by *daf-18*, a homologue of the tumour suppressor PTEN. Curr. Biol. *9*, 329–332.

Sarbassov, D.D., Guertin, D.A., Ali, S.M., and Sabatini, D.M. (2005). Phosphorylation and regulation of Akt/PKB by the rictor-mTOR complex. Science *307*, 1098–1101.

Sasaoka, T., Wada, T., and Tsuneki, H. (2006). Lipid phosphatases as a possible therapeutic target in cases of type 2 diabetes and obesity. Pharmacol. Ther. *112*, 799–809.

Savage-Dunn, C. (2005). TGF-beta signaling. In WormBook, The *C. elegans* Research Community, ed. 10.1895/wormbook.1.22.1, http://www.wormbook.org.

Smith, U., Axelsen, M., Carvalho, E., Eliasson, B., Jansson, P.A., and Wesslau, C. (1999). Insulin signaling and action in fat cells: associations with insulin resistance and type 2 diabetes. Ann. N Y Acad. Sci. *892*, 119–126.

Srinivasan, M., and Begum, N. (1994). Regulation of protein phosphatase 1 and 2A activities by insulin during myogenesis in rat skeletal muscle cells in culture. J. Biol. Chem. *269*, 12514–12520.

Stiernagle, T. (2006). Maintenance of *C. elegans*. In WormBook, The *C. elegans* Research Community, ed. 10.1895/wormbook.1.101.1, http://www.wormbook.org.

Stiles, B., Gilman, V., Khanzenzon, N., Lesche, R., Li, A., Qiao, R., Liu, X., and Wu, H. (2002). Essential role of AKT-1/protein kinase B alpha in PTEN-controlled tumorigenesis. Mol. Cell. Biol. *22*, 3842–3851.

Tang, X., Guilherme, A., Chakladar, A., Powelka, A.M., Konda, S., Virbasius, J.V., Nicoloro, S.M., Straubhaar, J., and Czech, M.P. (2006). An RNA interference-based screen identifies MAP4K4/NIK as a negative regulator of PPARgamma, adipogenesis, and insulin-responsive hexose transport. Proc. Natl. Acad. Sci. USA *103*, 2087–2092.

Testa, J.R., and Bellacosa, A. (2001). AKT plays a central role in tumorigenesis. Proc. Natl. Acad. Sci. USA *98*, 10983–10985.

Tesz, G.J., Guilherme, A., Guntur, K.V., Hubbard, A.C., Tang, X., Chawla, A., and Czech, M.P. (2007). Tumor necrosis factor alpha (TNFalpha) stimulates Map4k4 expression through TNFalpha receptor 1 signaling to c-Jun and activating transcription factor 2. J. Biol. Chem. *282*, 19302–19312.

Toker, A., and Newton, A.C. (2000). Akt/protein kinase B is regulated by autophosphorylation at the hypothetical PDK-2 site. J. Biol. Chem. *275*, 8271–8274.

Toker, A., and Yoeli-Lerner, M. (2006). Akt signaling and cancer: surviving but not moving on. Cancer Res. *66*, 3963–3966.

Ugi, S., Imamura, T., Maegawa, H., Egawa, K., Yoshizaki, T., Shi, K., Obata, T., Ebina, Y., Kashiwagi, A., and Olefsky, J.M. (2004). Protein phosphatase 2A negatively regulates insulin's metabolic signaling pathway by inhibiting Akt (protein kinase B) activity in 3T3-L1 adipocytes. Mol. Cell. Biol. *24*, 8778–8789.

Vowels, J.J., and Thomas, J.H. (1992). Genetic analysis of chemosensory control of dauer formation in *Caenorhabditis elegans*. Genetics *130*, 105–123.

Watson, R.T., Kanzaki, M., and Pessin, J.E. (2004). Regulated membrane trafficking of the insulin-responsive glucose transporter 4 in adipocytes. Endocr. Rev. *25*, 177–204.

Wolff, S., and Dillin, A. (2006). The trifecta of aging in *Caenorhabditis elegans*. Exp. Gerontol. *41*, 894–903.

Wolkow, C.A., Munoz, M.J., Riddle, D.L., and Ruvkun, G. (2002). Insulin receptor substrate and p55 orthologous adaptor proteins function in the *Caenorhabditis elegans daf-2*/insulin-like signaling pathway. J. Biol. Chem. *277*, 49591–49597.

Zdychova, J., and Komers, R. (2005). Emerging role of Akt kinase/protein kinase B signaling in pathophysiology of diabetes and its complications. Physiol. Res. *54*, 1–16.